Appl. Phys. A 83, 49–52 (2006)
DOI: 10.1007/s00339-005-3476-x

Applied Physics A
Materials Science & Processing

I.H. CHOWDHURY[1]
X. XU[1,✉]
A.M. WEINER[2]

Ultrafast two-color ablation of fused silica

[1] School of Mechanical Engineering, Purdue University, West Lafayette, IN 47907, USA
[2] School of Electrical and Computer Engineering, Purdue University, West Lafayette, IN 47907, USA

Received: 31 August 2005/Accepted: 23 November 2005
Published online: 17 January 2006 • © Springer-Verlag 2005

ABSTRACT Two ultrafast laser pulses at the fundamental Ti:sapphire laser wavelength of 800 nm and the second harmonic at 400 nm were used to study the temporal evolution of the transmissivity in fused silica and resulting material ablation. It was observed that there was a sharp drop in the transmissivity of the probe pulse at zero delay between the two pulses, indicating that there was enhanced absorption/reflection due to the creation of defect states or free electron plasma by the pump pulse. Subsequent atomic force microscopy measurements of the ablated holes revealed that the ablated volume increased by about 50% when the separations of the two pulses are within 300 fs. Two-color machining of channels at the surface also showed a similar increase in the machined depth and width when the pulses are overlapped in time.

PACS 52.38.Mf; 78.47.+p; 79.20.Ds

The use of ultrafast laser pulses for machining wide band-gap dielectrics, materials that are normally transparent to visible or near-infrared light, has been widely studied in recent years. The extremely high peak intensities that these amplified ultrafast pulses can achieve drive nonlinear absorption processes due to tunneling, multiphoton, and avalanche ionization. Several comprehensive reviews of the topic can be found in the literature [1, 2]. Recent studies [3, 4] have revealed the temporal dynamics of the absorption processes, showing the creation of dense free electron plasma and also rapid structural change at the surface on the order of a few picoseconds.

A related issue is the investigation of the type of defect-related absorption states that might contribute to enhanced absorption of the ultrafast laser pulses. To understand these phenomena better, it is useful to undertake pump-probe studies at different wavelengths to complement the existing literature. Also, using higher energy photons can help in exciting electrons from the valence band to intermediate states which can easily absorb light from the fundamental wavelength to cross the band-gap. Such a process has been reported in fused silica [5]. Two different nanosecond lasers were used in that study – a VUV F_2 laser at 157 nm (7.9 eV) and an UV KrF excimer laser at 248 nm (5 eV). A combination of the VUV and the UV photons are enough to excite an electron to the conduction band. This two-step process has been shown to be very efficient and is much more cost-effective than using the F_2 laser alone for ablation as the output power of this laser is quite low.

The amplified femtosecond laser has a high enough intensity to photoexcite electrons by multiphoton and tunneling ionization. However, it would be interesting to see if the use of both the fundamental 800 nm and the second harmonic 400 nm photons together could lead to enhanced absorption due to defect related energy states. Some work similar to this has been reported in the literature. A combination of the fundamental and second-harmonic beams of a Ti:sapphire laser were used to ablate polyethylene (PE) samples [6]. It was found that using a small amount of the second-harmonic beam at 395 nm (2 mJ/cm^2) along with 78 mJ/cm^2 of the fundamental at 790 nm led to a 12-fold enhancement in the etch depth as compared to the case where only the fundamental beam was used. However, this study did not look at the temporal dynamics of the modification process and no mention was made of the temporal separation of the 790 nm and 395 nm pulses during the course of the experiment. Another similar study was reported [7] where a combination of 180 fs pulses centered at 800 nm and 15 ns pulses at 532 nm were used to ablate fused silica and quartz samples. It was found that when the nanosecond pulse was delayed by about 30 ns behind the femtosecond pulse, the ablated volume increased by a factor of about two. This phenomenon was attributed the creation of free electrons and defect states by the femtosecond pulse which could be exploited by the longer pulse.

The experimental setup used in this study has a conventional pump-probe geometry that has been described in detail in a previous article [4]. In brief, 90 fs FWHM pulses centered at 800 nm produced by a Spectra-Physics Spitfire regenerative amplifier are separated by a beamsplitter and sent along two separate paths. One path has an adjustable delay while the other one is fixed. A type-I phase-matched BBO crystal was inserted in the delay arm to generate the second-harmonic pulse at 400 nm. Both the pulses were focused onto the sample with a long-working-distance Mitutoyo objective (10×, 0.28 NA). The transmitted light after the sample was

✉ Fax: +1-765/494-0539, E-mail: xxu@ecn.purdue.edu

collected with another objective (50×, 0.5 NA). Appropriate color filters were placed in front of the photo-detector measuring the transmissivity after the collecting objective to detect either 400 or 800 nm wavelengths, as necessary. All the results reported here, except the channel machining data, were collected in single-shot mode to avoid any possible incubation effects [8]. BBO has an inverse group-velocity mismatch (GVM) value of $\beta = 194$ fs/mm [9]. Using a sum of squares approximation, the 400 nm pulses produced in the 0.5 mm thick BBO crystal were estimated to have a longer pulsewidth of about 132 fs. Both pulses are focused to the sample surface with a diameter of about 4 μm. All experiments were conducted in air at atmospheric pressure. The samples used were 1 mm thick fused silica (Corning 7980) which were first cleaned with acetone and methanol.

One concern was the effect of chromatic aberration due to the fact that the same objective lens was used to focus both the 800 nm and 400 nm pulses. In order to test this, single-shot Z-scan [10] measurements were performed on the sample. Measurements were taken at both 400 nm and 800 nm separately with equal energies of about 0.4 μJ/pulse in both cases. It was found that both wavelengths showed very similar z-dependence of the transmissivity across the sample surface. The data are not reproduced here in the interests of brevity. As such, it can be assumed that the 800 nm and 400 nm pulses were well-overlapped at the focal position. Next, pump-probe transmissivity experiments were conducted on the fused silica sample. Both the 800 nm and the 400 nm pulses were used as probes alternately and the results are shown in Figs. 1 and 2, respectively. In this study, both the pump and probe pulses have comparable energies, which is in contrast to the usual convention wherein the probe is much weaker than the pump. We define the probe as the pulse whose transmissivity is measured by the detector. In all the plots, positive delay corresponds to the case where the probe comes after the pump and vice versa for negative delay. The maximum energy in the 400 nm beam that could be delivered to the sample was about 0.4 μJ because of constraints in how much 800 nm energy could be used to pump the BBO crystal and also the loss due to reflectivity of the mirrors and beamsplitters in the optical path. Much higher energies could be delivered at 800 nm and this beam was used to carry out the actual ablation while the 400 nm beam was used to only modify the dynamic absorption characteristics.

Figure 1 shows time-resolved transmissivity of an 800 nm probe pulse at 0.47 μJ at three different 400 nm pump energy levels (in μJ). Figure 2 shows time-resolved transmissivity of a 400 nm probe pulse at 0.4 μJ at four different 800 nm pump energy levels (in μJ). It is seen from Figs. 1 and 2 that both sets of data display a drop in the transmissivity near zero delay due to the creation of free carriers or defect states by the pump pulse. The feature that distinguishes the two plots is the fact that there is a rapid (∼ 1 ps) recovery in Fig. 1 but not in Fig. 2. Comparing transmissivity obtained at the same pump energy level of 0.4 μJ (the lowest level in Fig. 2), we see a complete recovery in transmissivity for the case of the 400 nm pump but not for the 800 nm pump. These can be explained in the following terms. The fast trapping seems to agree with previous reports in the literature that the free carriers in fused silica are trapped very

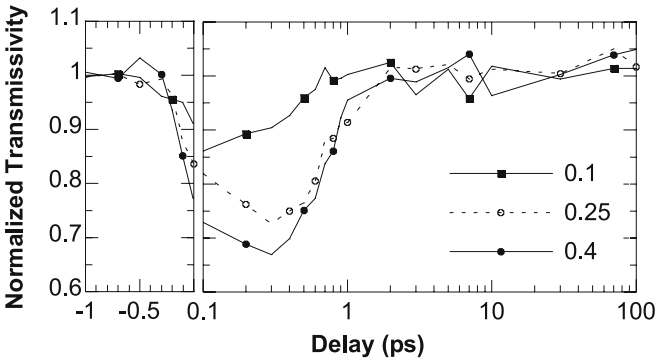

FIGURE 1 Time-resolved transmissivity of an 800 nm probe pulse at 0.47 μJ at three different 400 nm pump energy levels (in μJ)

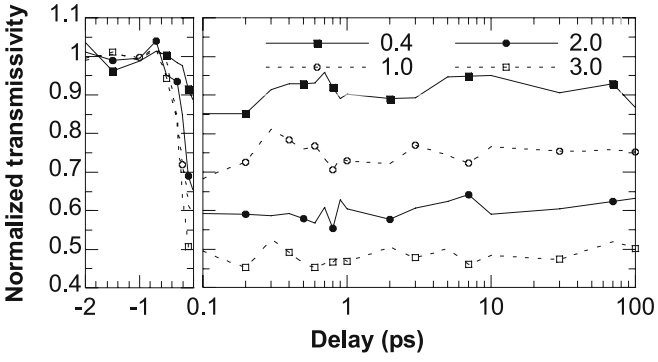

FIGURE 2 Time-resolved transmissivity of a 400 nm probe pulse at 0.4 μJ at four different 800 nm pump energy levels (in μJ)

rapidly due to the formation of self-trapped excitons (STEs) with a time constant of about 150 fs [11]. These STEs exhibit transient absorption bands at 4.2 eV and 5.2 eV and luminescence bands at 2.5 eV and 2.8 eV [12]. These are energy levels that can be accessed more easily by the higher energy 400 nm photons than by 800 nm photons. Also, previous studies [13] have identified defect states in fused silica, such as the non-bridging oxygen hole center (NBOHC) at 2.0 eV and the Si E′ center at 5.6 eV. It is possible that the 400 nm pump creates these defect states which are not accessible by the 800 nm (1.5 eV) photons. On the other hand, the defect states created by the 800 nm pump might easily absorb the 400 nm (3.1 eV) probe photons, especially if they are at NBOHC-type levels.

At the higher pump energy levels (1.0 μJ and above) shown in Fig. 2, the transmissivity stays at a lower level. This is due to the fact that at these pump energy levels, there is permanent surface damage, which reduces the transmissivity of the probe pulse. This has also been seen in previous 800 nm pump – 800 nm probe experiments [3, 4]. Under the focusing conditions employed in this experiment, the focal spot size is about 4 μm which yields a damage threshold for fused silica of 5.5×10^{13} W/cm^2 at 800 nm [4]. This corresponds to an energy value of about 0.62 μJ/pulse. Damage at 400 nm was found to occur at a lower energy level of about 0.4 μJ/pulse. Note in all the experiments, the transmission data are normalized with respect to the transmission of the probe at long negative delay; therefore, the self absorption effect of the probe pulse is already included in these data.

In order to take advantage of the enhanced absorption that should accompany the decrease in transmissivity seen in the pump-probe experiments in Fig. 1, two-color ablation experiments were conducted. The results of ablation volume together with the transmission data are shown in Fig. 3. The experiments were done with a single 800 nm pulse at 1.0 μJ and with a 400 nm pulse at 0.4 μJ placed at varying delay times before it. In this plot, positive delay corresponds to the 800 nm pulse coming after the 400 nm pulse. The transmissivity of the 800 nm pulse is measured. All the data-points shown in Fig. 3 are averaged over three experiments. A single 800 nm pulse at 1.0 μJ ablates about 0.47 μm^3 of material while a single 400 nm pulse at 0.4 μJ ablates a volume of about 0.02 μm^3 under the focusing conditions employed in this experiment. The corresponding maximum depths are 305 nm and 38 nm, respectively. When two pulses are used, the ablation volume varies with the time delay between the two pulses. There is an increase in the ablation volume at zero time delay as shown in Fig. 3, which corresponds to the transmissivity dip at zero delay. Up to delays of about 300 fs, the ablated volume exceeds the volume ablated by a single 800 nm pulse by about 50%. This enhancement in ablation is due to the increased absorption of the 800 nm pulse which follows the 400 nm pulse due to the creation of defect states or free electron plasma by the 400 nm pulse. However, an exact correlation of ∼ 50% increases in ablation with the ∼ 40% decreases in transmissivity is not possible because of two reasons. Firstly, the ablation rate is not linearly related to the absorbed energy. Secondly, the drop in transmissivity indicates an increase in absorption but an exact energy balance is not possible since reflected and scattered light is not measured in this study.

When the 0.4 μJ case in Fig. 1 is compared with the transmissivity data in Fig. 3, it is seen that the latter has a longer-lived drop. This is attributed to the fact that the 800 nm pulse energy used in Fig. 3 is much higher (1.0 μJ as compared to 0.47 μJ in Fig. 1). As such, nonlinear absorption mechanisms that occur at higher energy or intensity levels could be enabled. The 800 nm (1.5 eV) photons can thus be absorbed in NBOHC (2 eV) or Si E' type defect levels (5.6 eV) and also in the 4.2 eV and 5.2 eV absorption bands of the STEs created by the 400 nm pre-pulse, which would not be possible under linear absorption. The transmissivity recovery also happens on a much slower time-scale than the ablation enhancement. This is attributed to the fact that ablation is primarily a surface phenomenon while the transmissivity drop is also affected by absorption in the bulk of the material. This is because the ionization front of the free carrier plasma created by the ultrafast laser pulse moves rapidly into the bulk of the sample [14]. As such, the surface effects happen on a faster time-scale than the bulk effects. A similar result was seen in 800 nm pump–800 nm probe experiments reported previously [4] wherein it was observed that time-resolved reflectivity measurements (which depend on the surface condition) showed a much more rapid decay than the transmissivity data.

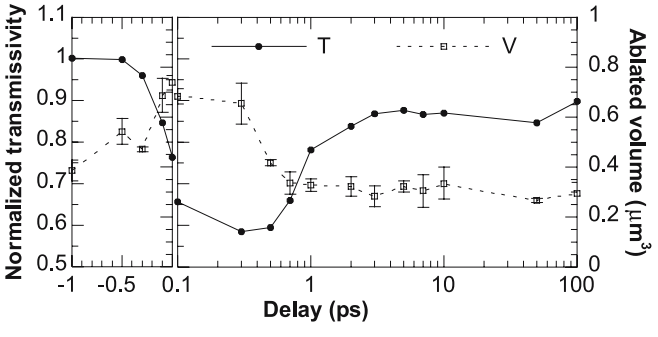

FIGURE 3 Time-resolved measurements of transmissivity and ablated volume for an 800 nm pulse at 1.0 μJ with a 400 nm pre-pulse at 0.4 μJ at different delays (T: transmissivity, V: ablated volume)

Another interesting feature of the experimental data is that the volume ablated at longer delays is actually slightly less than that ablated by a single 800 nm pulse. The AFM pictures show that the 400 nm pulse causes some surface roughening due to a small amount of ablation (∼ 38 nm crater depth). This might increase the scattering of the 800 nm pulse and thus reduce the energy coupling. It is also noted that the transmission is not fully recovered, which is due to scattering caused by the surface roughening.

Further verification of the increase in ablation is shown in Fig. 4 which shows a microscope picture of the array of holes machined at different delays. These holes are the same as the ones whose AFM-measured volume were plotted in Fig. 3. Again, positive delay implies that the 800 nm pulse follows the 400 nm one. It is seen that the holes machined at zero delay are larger than those machined at longer delays and also those machined with only a single 800 nm pulse at the same energy. The holes machined at longer delays tend to be smaller, displaying the same trend as the AFM measurements discussed in the previous paragraph. Also, channels were machined with the 1 kHz output of the regenerative amplifier by scanning the sample at a speed of 20 μ/s. The channel at the top in Fig. 5a was machined with a combination of 400 nm pulses at 0.1 μJ and 800 nm pulses at 1.0 μJ with zero delay between the pulses. The channel at the bottom was machined with only 800 nm pulses at 1.0 μJ. Machining with only the 400 nm, 0.1 μJ pulses produced no visible damage under microscope. It is seen from the figure that the channel at the top is wider than the one at the

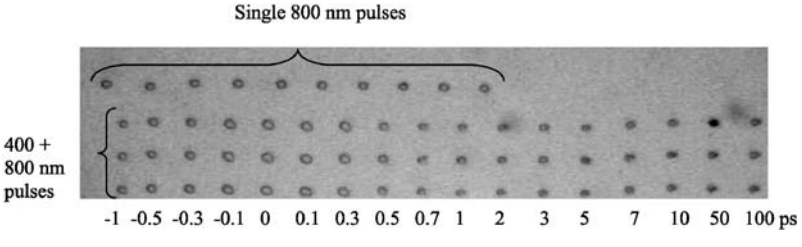

FIGURE 4 Optical micrograph of ablated holes in fused silica (numbers at the *bottom* indicate delay between 800 nm and 400 nm pulses in picoseconds)

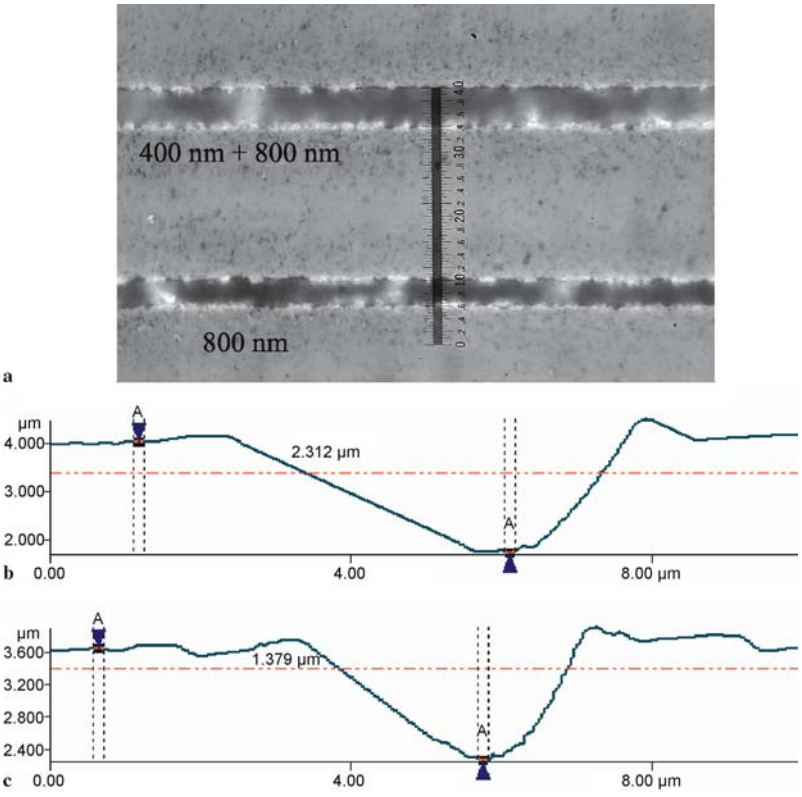

FIGURE 5 (**a**) Optical micrograph of channels machined in fused silica at a scanning speed of 20 μ/s (scale: 1.0 = 10.0 μm). AFM scans of the cross-section of the channel machined with (**b**) 800 nm and 400 nm pulses, and (**c**) only 800 nm pulses

bottom with nominal widths of about 6 μm and 4 μm, respectively. Also, AFM measurements shown in Fig. 5b and c reveal that they had maximum depths of about 2.3 μm and 1.4 μm, respectively. This result corresponds well to the single-shot data, which also showed an increase in ablated volume near zero delay between the 800 nm and 400 nm pulses.

The single-shot pump-probe experiments reported here show clearly that there is a temporal delay window during which enhanced absorption of the second pulse is possible. This is due to creation of free carriers and defect states by the preceding pulse which enhance energy absorption of the second pulse. This enhancement in absorption translates directly into an increase in the ablated volume when the pulses are separated within a certain delay time. These results suggest that using a combination of the fundamental and the second harmonic beams might allow us to exploit enhanced absorption effects for higher ablation rates.

ACKNOWLEDGEMENTS Support to this work by the National Science Foundation (DMI-0300488) is gratefully acknowledged.

REFERENCES

1 C.B. Schaffer, A. Brodeur, E. Mazur, Meas. Sci. Technol. **12**, 1784 (2001)
2 S.S. Mao, F. Quéré, S. Guizard, X. Mao, R.E. Russo, G. Petite, P. Martin, Appl. Phys. A **79**, 1695 (2004)
3 I.H. Chowdhury, X. Xu, A.M. Weiner, Appl. Phys. Lett. **86**, 151 110 (2005)
4 I.H. Chowdhury, A.Q. Wu, X. Xu, A.M. Weiner, Appl. Phys. A **81**, 1627 (2005)
5 K. Sugioka, K. Obata, M.H. Hong, D.J. Wu, L.L. Wong, Y.F. Lu, T.C. Chong, K. Midorikawa, Appl. Phys. A **77**, 251 (2003)
6 M. Okoshi, N. Inoue, Appl. Phys. A **79**, 841 (2004)
7 F. Théberge, S.L. Chin, Appl. Phys. A **80**, 1505 (2005)
8 M. Lenzner, J. Krüger, W. Kautek, F. Krausz, Appl. Phys. A **69**, 465 (1999)
9 F. Dmitriev, G.G. Gurzadyan, D.N. Nikogosyan, *Handbook of Nonlinear Optical Crystals* (Springer, New York 1997)
10 P.B. Chapple, J. Staromlynska, J.A. Hermann, T.J. McKay, J. Nonlinear Opt. Phys. **6**, 251 (1997)
11 F. Quéré, S. Guizard, P. Martin, G. Petite, O. Gobert, P. Meynadier, M. Perdrix, Appl. Phys. B **68**, 459 (1999)
12 C. Itoh, K. Tanimura, N. Itoh, J. Phys. C: Solid State Phys. **21**, 4693 (1988)
13 P.N. Saeta, B.I. Greene, Phys. Rev. Lett. **70**, 3588 (1993)
14 B.-T.V. Vu, O.L. Landen, A. Szoke, Phys. Plasmas **2**, 476 (1995)